PCCP

RSC Publishing

PAPER

View Article Online
View Journal

Products of the quenching of NO A $^2\Sigma^+$ (v = 0) by N_2O and CO_2

Cite this: DOI: 10.1039/c2cp43878j

Maximiliano A. Burgos Paci,[a] Julian Few,[b] Sarah Gowrie[b] and Gus Hancock*[b]

Collisional quenching of NO A $^2\Sigma^+$ (v = 0) by N_2O and CO_2 has been studied through measurements of vibrationally excited products by time resolved Fourier transform infrared emission. In both cases vibrationally excited NO X $^2\Pi$ (v) is seen and quantified in levels $v \geq 2$ with distributions which are close to statistical. However the quantum yields to produce these levels are markedly different for the two quenchers. For CO_2 such quenching accounts for only *ca.* 26% of the total: for N_2O it is *ca.* 85%. Far more energy is seen in the internal modes of the CO_2 product than those of N_2O. The results are rationalised in terms of cleavage of the N_2–O bond being dominant in the latter case, with either a similar O atom production or a specific channel producing almost exclusively NO in low vibrational levels (v = 0,1) for quenching by CO_2. Minor reactive channels yielding NO_2 are seen in both cases, and $O(^1D)$ is observed with low quantum yield in the reaction with N_2O. The results are discussed in terms of previous models of the quenching processes, and are consistent with the very high yield of NO X $^2\Pi$ (v = 0) previously observed by laser induced fluorescence for quenching of NO A $^2\Sigma^+$ (v = 0) by CO_2.

Received 1st November 2012,
Accepted 20th December 2012

DOI: 10.1039/c2cp43878j

www.rsc.org/pccp

Introduction

Nitric oxide is an important molecule in both atmospheric and combustion chemistry and observations on its γ band (A $^2\Sigma^+$–X $^2\Pi$) have been widely used for spectroscopic diagnostics in a variety of photochemical, gas discharge and combustion systems. Laser induced fluorescence (LIF) has often been the technique of choice.[1] At atmospheric pressures and above, typical of a combustion environment, measurements are often performed under conditions where collisional quenching processes are fast enough to return molecules to the probed state during the excitation pulse, and thus the outcome of such quenching processes needs to be understood for accurate interpretation of the measurements. As well as this practical importance the understanding of the dynamics of the quenching mechanisms is of fundamental interest. Many studies have been reported on the rates of NO A $^2\Sigma^+$ quenching by numerous colliders, and at a range of temperatures,[2–15] but what is still largely unknown is the fate of the electronic energy – how it is partitioned into the degrees of freedom of the colliding species, and whether or not reactive quenching takes place. One study which has addressed this question, specifically for tackling the problem of repopulation of the probed ground state by LIF, has been reported by Settersten *et al.*[16] who used LIF to probe the quantum yield of ground state NO X $^2\Pi$ (v = 0) formed by quenching of NO A $^2\Sigma^+$ (v = 0) by H_2O, CO, CO_2 and O_2. The results suggested that this channel accounts for ~30% of the quenching collisions for CO, H_2O and O_2, and for CO_2 a much larger fraction, 60%. This contrasts with the theoretical predictions based on collision complex or charge transfer models, where, as discussed later, the vibrational distributions will be statistical or peaked at low (but not zero) vibrational levels respectively.

The work by Settersten *et al.*[16] provided data only upon the ground vibrational level v = 0 of NO X $^2\Pi$. In contrast our own work[17] on the self-quenching of NO A $^2\Sigma^+$ (v = 0) used time-resolved Fourier Transform Infrared (FTIR) emission spectroscopy, which allowed the energy distributions in NO X $^2\Pi$ (v) to be measured over a wide range of vibrationally excited levels v. It was found that quenching by NO populates higher vibrational levels than fluorescence and emission was observed up v = 20, and this high vibrational level corresponds to 80% of the available energy appearing in NO vibration. The work presented here extends this type of study to the collisional quenching of NO A $^2\Sigma^+$ (v = 0) by N_2O and CO_2 and aims to determine how much of the available energy in the A state of NO, 529 kJ mol^{-1}, appears as vibrational excitation in the ground state NO molecule, whether or not the energy appears as internal excitation of the quenching molecule itself and if there is a contribution

[a] Universidad Nacional de Córdoba, INFIQC CONICET, Córdoba, Argentina
[b] Department of Chemistry, Oxford University, Physical and Theoretical Chemistry Laboratory, South Parks Road, Oxford OX1 3QZ, UK. E-mail: gus.hancock@chem.ox.ac.uk

from reactive quenching. We present nascent vibrational populations in NO X $^2\Pi$ (v), and show that there are very different degrees of vibrational excitation in the two collision partners, with evidence for a substantial contributions from reactive quenching in collisions with both CO_2 and N_2O.

Experimental

The technique of time-resolved FTIR Emission Spectroscopy has been described in several reviews[18–20] and only the basic methodology is summarized here. Radiation of wavelength around 226 nm from a frequency doubled pulsed tuneable dye laser (SIRAH PRSC-LG-24, 2 mJ pulse^{-1}, 10 Hz, pumped by a Quanta-Ray PRO-290-30 Nd:YAG laser) was directed into a stainless steel reaction vessel equipped with a multi-pass mirror system (6 passes of the UV beam) and Welsh collection optics for the resulting IR emission. The laser was normally tuned to the Q_{11} band head of the A $^2\Sigma^+$–X $^2\Pi$ (0,0) transition of NO at 226.257 nm and, following collisions with a chosen partner, IR emission from NO X $^2\Pi$ (v) and other products was observed. This emission was directed by a pair of parabolic mirrors into an FTIR spectrometer operating in step-scan mode (Bruker IFS/66), and detected generally with an InSb (Graseby IS-2) detector, operating in the range 1–5.5 μm. This range encompasses the first overtone spectrum ($\Delta v = -2$) of NO, and the strong $\Delta v_3 = -1$ bands of CO_2 and N_2O. In particular, the vibrational distributions for $v \geq 2$ in NO are very conveniently extracted from the well structured first overtone transitions,[17] and we use this emission to quantify the populations in NO X $^2\Pi$ $v \geq 2$. The IR wavelength range was extended to *ca.* 9 μm by means of a less sensitive HgCdTe detector. The step-scan method is similar to standard FTIR spectroscopy, but the path difference in the interferometer is moved in discrete steps, rather than scanned continuously. At each step, infrared emission is recorded as a function of time after the laser pulse to produce a series of interferograms, which then undergo Fourier Transformation to produce time-resolved spectra. The resulting spectra can then be used, for example in the determination of vibrational state distributions, energy transfer rates, product identities and branching ratios. In most of the experiments described here, 50 Torr of Ar was present in the reaction chamber to ensure rotational thermalisation without affecting the nascent product vibrational distributions. NO (supplied by MG Gases, purity > 99.5%) was passed through an acetone/dry ice slush bath (−78 °C) to remove any trace amounts of NO_2 present and its purity confirmed with IR absorption spectroscopy. CO_2 (BOC > 99.995%), N_2O (BOC > 99.995%) and Ar (BOC > 99.9995%) were used directly from the cylinders without further purification.

Results

Both CO_2 and N_2O are rapid electronic quenchers of NO A $^2\Sigma^+$ ($v = 0$), with rate constants of $\sim 4 \times 10^{-10}$ cm^3 molecule^{-1} s^{-1},[2,4,8,9,11,13–15] but are considerably slower at vibrational relaxation of NO X $^2\Pi$ (v). For both molecules, the vibrational quenching rate constants increase monotonically with increasing v with the highest reported value for N_2O, for quenching of $v = 12$, being 1.6×10^{-13} cm^3 molecule^{-1} s^{-1},[21] three orders of magnitude slower than electronic quenching, and a very similar value has been measured for the same v in quenching by CO_2.[22] Early time observations should thus enable nascent populations in NO X $^2\Pi$ (v) produced by electronic quenching to be observed before substantial vibrational relaxation takes place. IR emission bands of N_2O and CO_2 have large A factors for their $\Delta v_3 = -1$ transitions near 2000 cm^{-1}, of the order of ten times that for the NO fundamental band, and this will aid in the identification of emission features resulting from energy transfer to them. The quenching process may also give rise to other vibrationally excited products, produced for example by dissociation of the collision partner.

Quenching by CO_2

Vibrational excitation of NO X $^2\Pi$ (v) is observed by emission in both the fundamental and overtone regions when a mixture of NO and Ar is irradiated near 226 nm. On addition of CO_2 these bands decreased in intensity, and a new features are observed, ascribed to emission from high vibrational levels of CO_2, most notably in the $\Delta v_3 = -1$ bands near 2000 cm^{-1}.

We first concentrate on the overtone region of emission from NO X $^2\Pi$ (v) between 2800 and 3800 cm^{-1}. Previous work has described the tests used to ensure that the observed IR emission is the result of collisional deexcitation of NO A $^2\Sigma^+$ ($v = 0$) and not from for example products of a two photon excitation step.[17] Fig. 1 shows vibrational overtone spectra recorded 10 μs after pumping 50 mTorr NO and 50 Torr Ar at 226.257 nm with and without CO_2, taken at a resolution of 20 cm^{-1}. For the NO/Ar mixture the vibrational levels are formed by

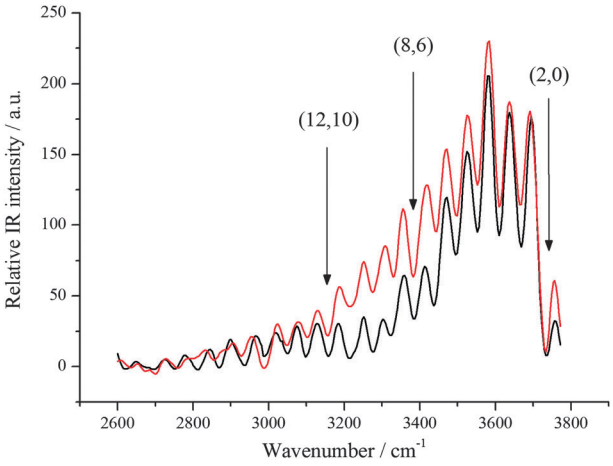

Fig. 1 NO X $^2\Pi$ ($\Delta v = -2$) emission spectrum recorded at 10 μs following excitation of 50 mTorr of NO X $^2\Pi$ in the Q_{11} bandhead of the NO A$^2\Sigma^+$ ($v = 0$) ← X $^2\Pi$ ($v = 0$) transition in the presence of 466 mTorr CO_2 ($\Phi_{CO_2} = 0.53$, red) and 50 Torr Ar at a resolution of 20 cm^{-1}. Shown also on this figure is the corresponding spectrum produced from fluorescence and self-quenching by NO, which has a Franck–Condon distribution for the low vibrational levels ($\Phi_{NO} = 0.08$, $\Phi_{CO_2} = 0$, black). Selected band origins are shown. In this figure the two spectra are arbitrarily scaled for clarity: the relative intensities are discussed in the text.

fluorescence at low v (with a quantum yield $\Phi = 0.92$) and self quenching at high v ($\Phi = 0.08$). Quantum yields are calculated from fluorescence decay rates[23,24] and self quenching rate constants.[2,8,11,12] A selection of band origins are marked on the figure. Also shown in Fig. 1 is a spectrum when 0.466 Torr CO_2 (quenching quantum yield $\Phi = 0.53$) is added, and it can be seen that the emission now stretches to higher vibrational levels. The quantum yield is calculated using measured rate constants for quenching by CO_2 which are generally in good agreement.[2,4,8,9,11,13–15] The emission in the NO overtone region was perturbed at early times by strong emission from two combination bands of vibrationally excited CO_2 ($\Delta v_3 = \Delta v_1 = -1$ and $\Delta v_3 = -1$, $\Delta v_2 = -2$), but the addition of Ar removed the emission within *ca.* 10 μs. Several NO overtone spectra were summed from 10–40 μs and fitted to a spectral simulation,[17] with the results averaged. The rates of vibrational relaxation of NO X $^2\Pi$ (v) by CO_2 under these conditions are negligible.[21]

The emission spectra presented in Fig. 1 have contributions from both NO self-quenching and fluorescence as well as from quenching by CO_2. To separate these contributions the spectra (which often were taken on different days) need to be placed upon a common intensity scale. Optical filters were used to isolate specific wavelength bands, and the intensities passed by the filter were measured with and without CO_2 on a timescale of a few minutes. These infrared intensities were scaled to the respective peak intensities of the simultaneously measured NO A–X (0,0) uv fluorescence in order to allow for any variation of laser intensity, and also for any change in the rotational hole filling during the excitation pulse brought about by a change of gas composition.[17] Such scaling showed that the addition of CO_2 resulted in a marked decrease of the overtone intensity. For example, emission through a filter centred at 3720 cm^{-1} passing radiation in the $2 \rightarrow 0$ to $5 \rightarrow 3$ bands was reduced by some 40% when the quantum yield of CO_2 quenching was increased from 0 to 0.53. Fig. 1 shows that addition of CO_2 results in a relative increase in populations of vibrational levels of NO X $^2\Pi$ (v = 5–12), and the increase in Einstein A coefficients of these higher levels would imply that if quenching produced exclusively NO X $^2\Pi$ (v) in the observed emitting levels by process (1)

$$\text{NO A } ^2\Sigma^+ (v = 0) + CO_2 \rightarrow \text{NO X } ^2\Pi (v) + CO_2 \qquad \Delta H^0_{298} = -529 \text{ kJ mol}^{-1} \quad (1)$$

then the overall overtone emission intensity should increase instead of decrease. However we need also to take into account three other potential reactive processes, neither of which form vibrationally excited NO X $^2\Pi$:

$$\text{NO A } ^2\Sigma^+ (v = 0) + CO_2 \rightarrow \text{NO X } ^2\Pi (v = 0) + CO + O(^3P) \qquad \Delta H^0_{298} = 3.2 \pm 0.4 \text{ kJ mol}^{-1} \quad (2)$$

$$\text{NO A } ^2\Sigma^+ (v = 0) + CO_2 \rightarrow NO_2 + CO \qquad \Delta H^0_{298} = -303 \pm 0.4 \text{ kJ mol}^{-1} \quad (3)$$

and

$$\text{NO A } ^2\Sigma^+ (v = 0) + CO_2 \rightarrow NCO + O_2 \qquad \Delta H^0_{298} = -76 \pm 14 \text{ kJ mol}^{-1} \quad (4)$$

Here we note that the occurrence of these three processes could result in a decrease in NO (v) emission intensity. We discuss these processes below, and we will term them ''unobserved channels'', where unobserved here refers to processes which either do not form NO, or produce NO exclusively in levels which are not seen in the overtone spectra.

The second step in the extraction of populations from process (1) is to take the normalised set of spectra and to subtract from each spectrum with CO_2 the spectrum without CO_2 multiplied by the appropriate quantum yield of fluorescence and self quenching (for example 0.47 in the data of Fig. 1). The resulting spectrum, now the result of CO_2 quenching alone, is fitted to obtain vibrational distributions. However we have no population from levels v = 0 and 1. We estimate these as before[17] from a Surprisal analysis of the data. A Surprisal plot compares the measured vibrational distribution, $P(f_v)$ where f_v is the fraction of the available energy appearing in vibrational level v, with that expected from a statistical distribution of the energy, $P^0(f_v)$ the so called ''Prior'' distribution.[25] A linear relationship of the form

$$\ln \frac{P(f_v)}{P^0(f_v)} = -\lambda_0 - \lambda_1 f_v \quad (5)$$

has been found for many reactive and photodissociative processes,[26,27] with a negative value of the Surprisal parameter λ_1 indicating a vibrational distribution which is hotter than statistical. If we assume such a relationship for the observed vibrationally excited levels, extrapolation can yield information on those not measured.

For collisions of NO A $^2\Sigma^+$ (v = 0) with CO_2, the only exothermic channel producing vibrationally excited NO X $^2\Pi$ (v) is the energy transfer process (1) and for this the Prior distribution is calculated by the methods outlined by Muckerman[28]

$$P^0(f_v) = N(1 - f_v)^{13/2} \quad (6)$$

where N is a normalisation factor. Fig. 2 shows the appropriate Surprisal plot of $\ln[P(f_v)/P^0(f_v)]$ against f_v for v = 3–14. For v = 2 the combination of a low Einstein A coefficient for the $(2 \rightarrow 0)$ transition and the strong CO_2 combination band emission at early time made the evaluation of the weak emission contribution from v = 2 unreliable, and thus we present data only for v = 3–14, and use an extrapolation for levels v = 0–2. The subtraction procedure resulted in populations in levels $v > 14$ which are thermodynamically possible for process (1) being zero within the noise of the experiment, and the reasons for this are discussed later. The Surprisal parameter λ_1, defined as the negative of the gradient of such a plot, is found to be 0.33 ± 0.14, indicating that the distribution although close to the Prior, shows that NO takes a marginally lower than statistical share of the available energy, 11.4% instead of the statistical 11.8%. The measured v = 3–14 populations and the extrapolated populations for v = 2, 1 and 0 are given in Table 1, summed to unity.

We now have the population distributions for the three processes occurring in data such as presented in Fig. 1, namely for CO_2 quenching (Table 1), NO self quenching[17] and fluorescence.[23,24]

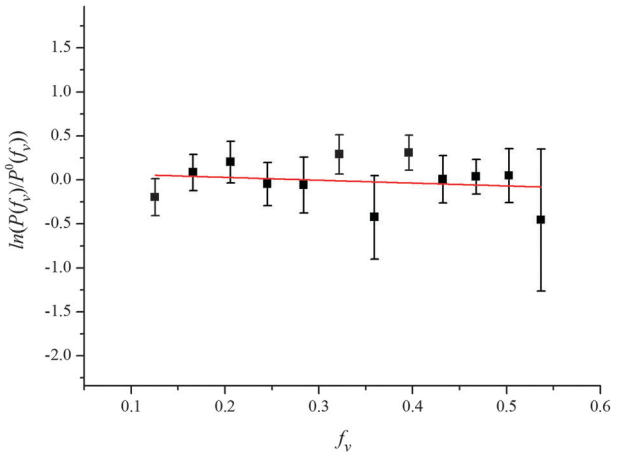

Fig. 2 A Surprisal plot of the nascent vibrational distributions of NO X $^2\Pi$ (v = 3–14) following pumping of 50 mTorr NO on the Q_{11} bandhead of the A $^2\Sigma^+$ (v = 0) ← X $^2\Pi$ (v = 0) transition and quenching by CO_2 (■). A linear fit to the data is also plotted, yielding a Surprisal parameter λ_1, defined as the negative of the gradient of such a plot, of 0.33 ± 0.14.

Table 1 Vibrational populations for NO X $^2\Pi$ (v = 0–14) produced under conditions of exclusive quenching by CO_2 from a combination of the experimental data for populations of NO X $^2\Pi$ (v > 2) and Surprisal analysis for the populations of NO X $^2\Pi$ (v = 0–2). Relative populations are summed to unity with errors presented as ±1σ

v	NO X $^2\Pi$ (v) vibrational population quenching by CO_2
0	0.250 ± 0.024
1	0.186 ± 0.023
2	0.137 ± 0.025
3	0.100 ± 0.021
4	0.098 ± 0.020
5	0.080 ± 0.019
6	0.045 ± 0.011
7	0.031 ± 0.010
8	0.031 ± 0.007
9	0.011 ± 0.005
10	0.015 ± 0.003
11	0.007 ± 0.002
12	0.005 ± 0.001
13	0.003 ± 0.001
14	0.001 ± 0.001

A check on the accuracy of the populations was carried out by using them to simulate an early time fundamental spectrum ($\Delta v = -1$) near 1800 cm^{-1} in the presence of CO_2. Although the spectrum at low resolution (20 cm^{-1}) has virtually no structure in comparison with that of the overtone and thus is less suitable for population determinations, excellent agreement between the simulation and the experimentally observed spectrum was found, which gives particular confidence in the estimation of the population in v = 2 where the overtone emission coefficient is low. For $v = 1 \rightarrow 0$ emission the fundamental band taken at high resolution showed evidence of self absorption (the weak Q branch lines were proportionally stronger than the R and P branches) and thus extracting the v = 1 population from an emission spectrum is unreliable. The populations in Table 1, together with the measured reduction in overtone intensity with increasing CO_2 concentrations enables us to deduce that process (1) forming the observed channels (*i.e.* $v \geq 2$) together with the extrapolated populations in v = 0,1, which we now call process (1a) accounts for 26 ± 5% of the removal of NO A $^2\Sigma^+$ (v = 0) in collisions with CO_2, implying that there are additional unobserved channels (74%) such as a separate mechanism forming unobserved NO (v = 0,1) by process (1b), or the reactive processes (2)–(4):

$$\text{NO A } ^2\Sigma^+ (v = 0) + CO_2 \rightarrow \text{NO X } ^2\Pi (v) + CO_2 \quad (1a)$$

$$\text{NO A } ^2\Sigma^+ (v = 0) + CO_2 \rightarrow \text{NO X } ^2\Pi (v = 0, 1) + CO_2 \quad (1b)$$

We note also that Table 1 shows the fractional population of v = 0 produced by process (1a) is 25%, which, with a 26% quantum yield would imply that process (1a) alone yields a ground state population in NO X $^2\Pi$ (v = 0) of 6.5% resulting from quenching by CO_2, far smaller than the figure of 60% deduced by Settersten *et al.*[16] from their LIF measurements. We discuss below the resolution of this difference.

Fig. 3 presents a contour plot of the infrared emission observed with the HgCdTe detector following irradiation of 50 mTorr NO at 226 nm in the presence of 46 mTorr CO_2 and 50 Torr Ar. The plot shows the wavelength dependence of the emission in the region 1250–3500 cm^{-1} with the intensity represented as contours of different colours. The conditions represent the case when collisional quenching by CO_2 has a quantum yield of $\Phi(CO_2)$ = 0.1. Three features are clearly seen. First, long lived emission between 1700–1850 cm^{-1} is in the position expected for the fundamental bands of NO produced with a vibrational distribution as given in Table 1. Vibrational relaxation of NO (v) is slow on the time scale shown in Fig. 3. Secondly, a stronger feature between 1800 and 2300 cm^{-1} is seen to cascade rapidly to higher wavenumbers with time and is assigned to highly vibrationally excited CO_2, formed directly by

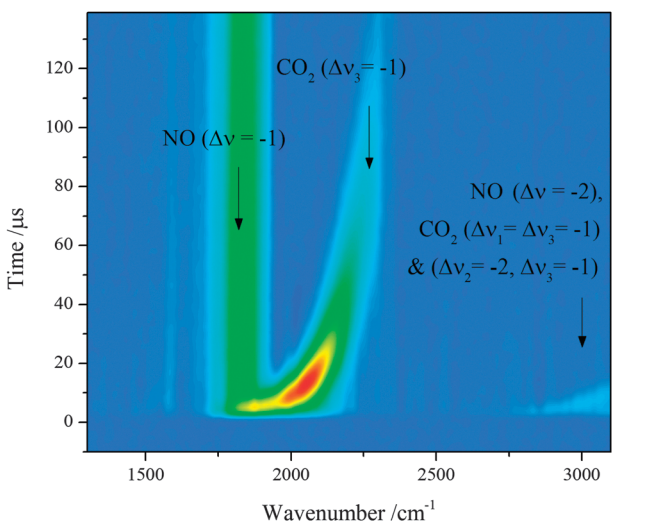

Fig. 3 Contour plot of IR emission spectrum recorded at a resolution of 20 cm^{-1} following the initial excitation of 50 mTorr NO to the NO A $^2\Sigma^+$ (v = 0) state in the presence of 50 Torr Ar and 46 mTorr CO_2 (Φ_{CO_2} = 0.1). This was acquired with a HgCdTe detector. Band assignments are marked. Red represents high intensity and blue represents low intensity.

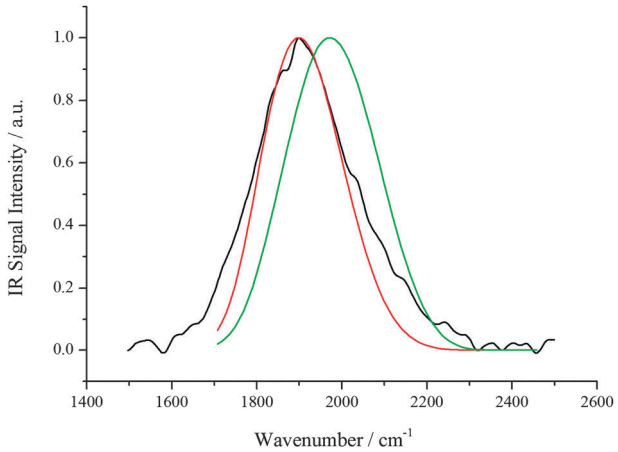

Fig. 4 IR emission spectrum recorded 4 μs after pumping 50 mTorr NO to the NO A $^2\Sigma^+$ ($v = 0$) state in the presence 46 mTorr CO_2 (black curve, $\Phi_{CO_2} = 0.1$). Also shown is simulated spectra predicted according to the best fit Surprisal parameter, $\lambda_1 = -6$ (red curve), as well as the simulated spectra from a statistical (Prior) distribution (green curve). The spectra are normalised for clarity.

energy transfer from NO A $^2\Sigma^+$ ($v = 0$) by process (1), emitting in $\Delta v_3 = -1$ transitions, and rapidly quenched in collisions with CO_2 and Ar. The third set of emission bands above $\sim$3000 cm^{-1}, is assigned to emission from the NO first overtone and (at early times) from combination bands of CO_2. In addition there is a weak feature near 1600 cm^{-1}, discussed later as being from vibrationally excited NO_2.

We observe no emission from CO_2 (0,0,1) → (0,0,0) even at late times because of self-absorption. Fig. 4 shows the intensity distribution of the CO_2 band at early times (4 μs) with the long lived NO fundamental emission subtracted. This spectrum was taken in the absence of Ar, as relaxation with 50 Torr Ar of the CO_2 levels of high vibrational excitation (the low wavenumbers in Fig. 4) was pronounced within the time scale of the experiments. The lack of structure and the wide wavenumber range of the band suggests that the CO_2 is formed over a range of vibrational states, CO_2 (v_1,v_2,v_3), which are not resolved in the spectra, making accurate extraction of populations by a simple spectral simulation difficult due to the large number of adjustable parameters. We first compare the observed spectrum with that for a Prior distribution for CO_2 in process (1), calculated, *via* the methods outlined previously, as[28]

$$P^0(v_1, v_2, v_3) = N(f_v)^3(1 - f_v)^{7/2} \quad (7)$$

where again f_v represents the fraction of the available energy in level (v_1,v_2,v_3), and N is a normalization factor. After calculating the values of P^0 for each possible combination of levels (v_1,v_2,v_3), each $\Delta v_3 = -1$ band from a given (v_1,v_2,v_3) level was represented by two (P and R branches with separation of *ca.* 25 cm^{-1}) or three (P, Q, R branches) lines representing transitions between levels with or without $\ell = 0$. Positions of band origins were calculated according to Herzberg[29] and several were confirmed by comparison with those measured by Bailly *et al.*[30] The intensity of each band was calculated using eqn (8)

$$I(v_1, v_2, v_3) = P^0(v_1, v_2, v_3)\left[\frac{\bar{\nu}(v_1, v_2, v_3)}{\bar{\nu}(0, 0, 1)}\right]^3 v_3 A_{001} N_{PQR} \quad (8)$$

where A_{001} is the Einstein A coefficient for the v_3 fundamental transition, $\bar{\nu}$ the frequency of the $\Delta v_3 = -1$ transition and N_{PQR} is a factor taking into account the relative intensities of P, Q and R branches. The cubic term allows for the dependence of the spontaneous emission coefficient on frequency, and the v_3 quantum number dependence assumes harmonic oscillator behaviour. Fermi resonance between v_1 and v_2 was considered for levels with $v_1 < 10$. The resulting simulated spectrum was then corrected for instrumental spectral response and is compared with the experimental spectrum in Fig. 4. It can be seen that the simulated spectrum for a Prior distribution peaks at higher wavenumbers than is observed experimentally, suggesting that the observed distribution is vibrationally hotter than statistical. A negative Surprisal parameter λ_1 shifts the peak of the calculated emission to lower wavenumbers as expected. Fig. 4 shows the fit obtained with $\lambda_1 = -6.0$, which simulates the observed peak, but gives a distribution narrower than observed. Vibrational mode specific Surprisal parameters have been used to model triatomic infrared emission where the simple analysis yielded distributions broader than observed,[31] but was not attempted in this present case because of the difficulty of finding a unique combination of the three adjustable parameters with confidence. What is clear however is that CO_2 takes a higher than statistical share of the available energy in process (1); a Surprisal parameter of −6.0 implies that the average vibrational energy in CO_2 is 62% of that available compared with 47% expected statistically.

We are able to dismiss the possibility of the emission arising from CO_2 and N_2O produced by reaction of NCO formed in process (4) with NO:

$$NCO + NO \rightarrow N_2 + CO_2 \quad (9a)$$

$$\rightarrow N_2O + CO \quad (9b)$$

The infrared emission arising from reactions (9a) and (9b) peaks at 2100 cm^{-1},[31] considerably shifted from that shown in Fig. 4. In addition, the present emission (both in the CO_2 fundamental and combination band regions) is always seen to be prompt, appearing with the rise time of the detector, of the order of 2–3 μs, whereas that from the reactive process (9) would be expected to have a rise time, calculated from the rate constant of 3.1×10^{-11} cm^3 $molecule^{-1}$ s^{-1},[31] to be an order of magnitude larger at 50 mTorr NO.

Fig. 5 shows a longer time (30 μs) spectrum, taken when the CO_2 emission has shifted to low vibrational levels near 2400 cm^{-1}. Here we see not only the relatively long lived NO fundamental band, but also a feature near 2100 cm^{-1}, and this is assigned to the CO ($v = 1 \rightarrow 0$) transition, confirmed by experiments in which a cold gas filter containing CO removed the emission entirely with very little effect on that from CO_2. The cold gas filter experiments also showed that the emission from CO ($v = 1$) was not prompt, in contrast to that from nascent NO and CO_2, and had a relatively long lifetime. Process (2) producing CO has been suggested by Settersten *et al.*[16] as a possible explanation for a surprisingly large cross section for quenching of NO A $^2\Sigma^+$ ($v = 0$) by CO_2. As can be seen for

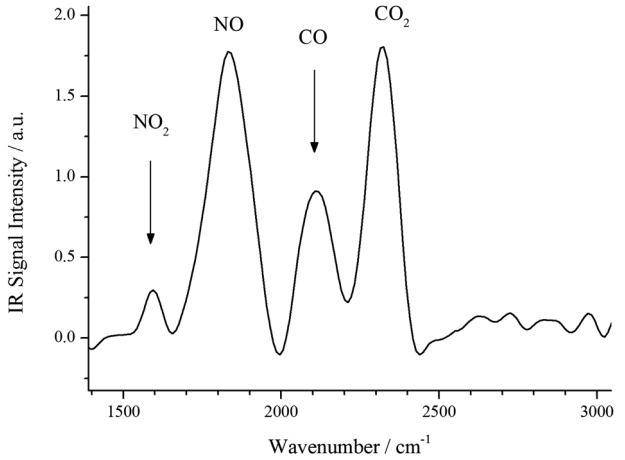

Fig. 5 An emission spectrum recorded 30 μs after excitation of 50 mTorr NO X $^2\Pi$ to the A $^2\Sigma^+$ (v = 0) state with 226.257 nm radiation in the presence of 4.3 Torr CO_2 and 50 Torr Ar. Spectra was recorded with a HgCdTe detector at 50 cm^{-1} resolution. Emission features are labeled.

process (2) at 298 K the reaction is slightly endothermic (ΔH^0_{298} = 3.2 kJ mol^{-1}), but becomes slightly exothermic at low temperatures ($\Delta H^0_0 = -3.0$ kJ mol^{-1}), which implies that the reaction is thermodynamically feasible for lower than room temperature distributions of the available energy in the products. Such a pathway however would produce NO and CO in their vibrational ground states, and thus the observed CO (v = 1) therefore cannot be formed directly. The emission intensity of CO (v = 1) was found to increase but with the same temporal behaviour following a prolonged period (3 hours) of 226 nm irradiation. The evidence suggests that it is not a nascent emitting product, but is presumably formed by efficient near resonant energy transfer to CO (v = 0) from vibrationally excited NO X $^2\Pi$ (v) or CO_2. Process (2) therefore could account for this observation, but an alternate option would be reaction (3) to produce CO together with NO_2. As can be seen in Fig. 3 and 5 we observe weak emission near 1600 cm^{-1} which we attribute to vibrationally excited NO_2 in the $\Delta v_3 = -1$ bands but the intensity is far lower than that from vibrationally excited NO in the fundamental region, despite the Einstein A coefficient for the (0,0,1) → (0,0,0) transition being approximately a factor of 10 greater than that for NO (v = 1 → 0).[32] If process (3) does occur, then it would need to produce a far lower quantum yield of vibrationally excited products than does process (1), both in NO_2 and CO. There is sufficient energy liberated in process (3) to populate CO up to v = 10, yet we see no emission from highly excited CO either in the fundamental or overtone regions. Although our observations cannot rule out process (3) as having a significant quantum yield, they support the process partitioning little energy into vibration of the products.

If we neglect processes (3) and (4), we can explain the observations as follows. CO_2 quenches NO A $^2\Sigma^+$ (v = 0) in process (1a) to produce NO X $^2\Pi$ (v) with a vibrational distribution close to statistical and with a quantum yield of 26 ± 5%. The remaining 74% of quenching collisions come from process (1b) forming unobserved NO X $^2\Pi$ (v = 0,1) or reaction in process (2) which can only produce NO in (v = 0), or a combination of the two. The CO_2 product comes from processes (1a) and (1b). The low quantum yield for process (1a) also helps to explain why its vibrational distribution obtained by subtraction yields negligible population in levels above v = 14. The vibrational distribution for NO self quenching[17] yields a Surprisal parameter of −2.16 ± 0.44, compared with the CO_2 quenching value of 0.33. Although these values are both close to statistical, the hotter NO quenching distribution and the smaller number of degrees of freedom available to the products in comparison with process (1a) means that quenching by NO will dominate the formation of high vibrational levels under the present conditions, and this effect is exacerbated by the reduced quantum yield of process (1a).

Quenching by N_2O

The addition of N_2O to the standard mixture of 50 mTorr NO in 50 Torr Ar irradiated at 226 nm causes a far smaller change in the intensity of the overtone emission from NO X $^2\Pi$ (v) than that produced by the addition of CO_2 reported earlier. Fig. 1 shows that CO_2 markedly increases the fraction of higher vibrational levels: for N_2O the change is in the opposite direction, *i.e.* as the quantum yield of quenching by N_2O is increased there is a decrease in the relative population of the high vibrational levels. This effect can be most clearly seen in a plot of the vibrational populations of NO X $^2\Pi$ (v) for v = 2–18 under conditions of low (Φ = 0.1) and high (Φ = 0.9) quantum yields of N_2O quenching shown in Fig. 6. In addition to the NO bands two other emission features are seen, between 2000 and 2300 cm^{-1}, and are shown in a contour plot of Fig. 7. Intense emission near 2200 cm^{-1} is seen to rise with time, and a weak feature appears near 2000 cm^{-1} (in this example a filter was used to block the NO fundamental bands below 1850 cm^{-1}). At higher wavenumbers in Fig. 7 the structured NO first overtone

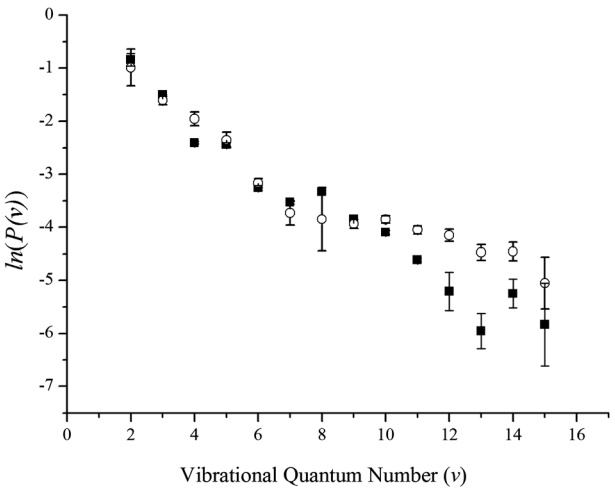

Fig. 6 Log plot of the averaged normalised nascent populations of NO X $^2\Pi$ (v = 2–15) following pumping of 50 mTorr NO to its A $^2\Sigma^+$ (v = 0) state in the presence of 50 Torr Ar and 43 mTorr (○, Φ_{N_2O} = 0.1) and 3.5 Torr (■, Φ_{N_2O} = 0.9) of N_2O. An error of ±1σ is shown.

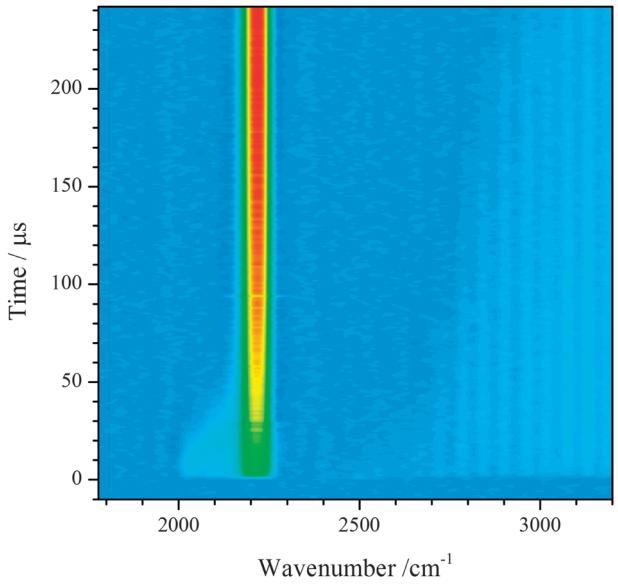

Fig. 7 Contour plot of spectra recorded with the InSb detector at a resolution of 20 cm^{-1} following pumping of 50 mTorr NO X $^2\Pi$ to its A $^2\Sigma^+$ ($v = 0$) state in the presence of 45 mTorr N_2O ($\Phi_{N_2O} = 0.1$) and 50 Torr Ar, using an optical filter to cut out intense emission from fundamental vibrational bands of NO. Red represents high intensity and blue represents low intensity.

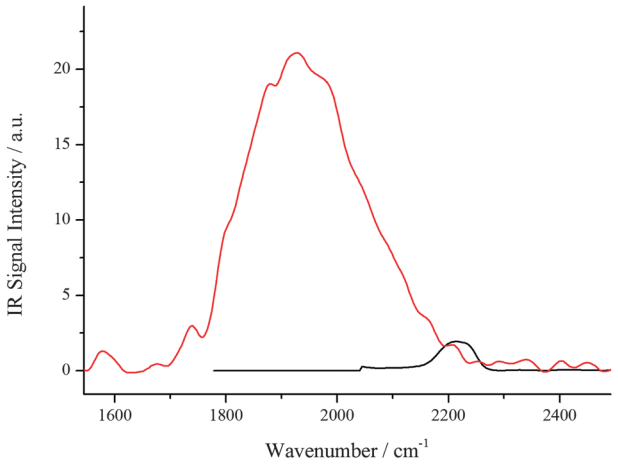

Fig. 8 IR emission spectrum recorded at a resolution of 20 cm^{-1} following the pumping of 50 mTorr NO on the Q_{11} bandhead of the NO A $^2\Sigma^+$ ($v = 0$) ← X $^2\Pi$ ($v = 0$) transition in the presence of 50 Torr Ar and either 46 mTorr CO_2 (red curve, $\Phi_{CO_2} = 0.1$) or 45 mTorr N_2O (black curve, $\Phi_{N_2O} = 0.1$). The plots have been scaled according an experiment where NO A $^2\Sigma^+$ ($v = 0$) was quenched by both N_2O and CO_2 with equal quantum yields. The NO X $^2\Pi$ ($\Delta v = -1$) signal (see for example Fig. 3) has been subtracted.

transitions are observable. The carrier of the strong and wavenumber invariant emission near 2200 cm^{-1} is clearly not a nascent product, and we consider it later. We first identify the 2000 cm^{-1} feature as emission from vibrationally excited N_2O formed in the direct energy transfer process

$$\text{NO A } ^2\Sigma^+ (v = 0) + N_2O \rightarrow \text{NO X } ^2\Pi (v) + N_2O \qquad \Delta H^0_{298} = -529 \text{ kJ mol}^{-1} \qquad (10)$$

as its behaviour (being rapidly formed in the position expected for emission in the $\Delta v_3 = -1$ bands of N_2O, and cascading to low vibrational levels as a function of time) mimics that of CO_2 formed in process (1). However, the major difference between the two added gases is the intensity of the $\Delta v_3 = -1$ emission bands, as a comparison of the relative intensities of these bands and the NO overtones in Fig. 3 and 7 indicates qualitatively. This is more clearly illustrated in Fig. 8 where early time spectra in the presence of 50 Torr Ar from both CO_2 and N_2O at the same quantum yields of quenching ($\Phi = 0.1$) are shown. In these spectra the fundamental $\Delta v = -1$ transitions of NO have been subtracted: this is a straightforward process, as the relaxation rates of the vibrationally excited levels of NO are far slower than those of CO_2 or N_2O, and thus a late time NO fundamental spectrum can be subtracted from the early time data (see for example Fig. 3). The Einstein A coefficients for the $\Delta v_3 = -1$ transitions in the two triatomic molecules are similar to within a factor of 2: for the (0,0,1) → (0,0,0) transitions the values are 340 s^{-1} for CO_2 and 195 s^{-1} for N_2O,[33] and it is clear that process (10) is far less efficient at populating vibrationally excited levels in the acceptor molecule than is process (1). We also note that the N_2O vibrational distribution peaks far more closely to its fundamental band (2223 cm^{-1}) than does that for CO_2 (2349 cm^{-1}).

Before we can extract NO X $^2\Pi$ (v) populations resulting from quenching by N_2O in the same way as described above for CO_2 we need to consider three other channels by which they can be formed. The relative weakness of the N_2–O bond makes the dissociative steps

$$\text{NO A } ^2\Sigma^+ (v = 0) + N_2O \rightarrow \text{NO X } ^2\Pi + N_2 \text{ X } ^1\Sigma_g^+ (v) + O(^3P) \qquad \Delta H^0_{298} = -361 \pm 0.6 \text{ kJ mol}^{-1} \qquad (11)$$

$$\text{NO A } ^2\Sigma^+ (v = 0) + N_2O \rightarrow \text{NO X } ^2\Pi (v) + N_2 \text{ X } ^1\Sigma_g^+ (v) + O(^1D) \qquad \Delta H^0_{298} = -173 \pm 0.6 \text{ kJ mol}^{-1} \qquad (12)$$

exothermic, in contrast with the corresponding process for CO_2. In addition the process forming ground state N(^{4}S) atoms becomes thermodynamically possible:

$$\text{NO A } ^2\Sigma^+ (v = 0) + N_2O \rightarrow 2\text{NO X } ^2\Pi (v) + N(^4S) \qquad \Delta H^0_{298} = -46.0 \pm 1 \text{ kJ mol}^{-1} \qquad (13)$$

Vibrationally excited NO X $^2\Pi$ (v) can therefore be formed in four possible processes, (10)–(13). The populations in the observed overtone levels are now treated as in the case for CO_2, with contributions from self quenching and fluorescence subtracted from the spectra according to their quantum yields, with the quenching rate constant for N_2O taken as the average of the two most recent measurements,[2,13] (4.7 ± 0.4) × 10^{-10} cm^3 $molecule^{-1}$ s^{-1}. Measured relative populations are shown in Table 2 for v = 2–14. We now calculate, as for the CO_2 case, the fraction of the quenching process with N_2O which leads to unobserved processes. For example an unobserved channel could be the exclusive formation of NO (v = 0 and 1) levels in one or more processes with NO ($v \geq 2$) produced

Table 2 Predicted vibrational populations for NO X $^2\Pi$ (v) with 100% quenching by N_2O produced by direct energy transfer to N_2O, as described by process (10), and also by the $O(^3P)$ channel as shown in process (11). These were determined from a combination of the experimental data for populations of NO X $^2\Pi$ ($v > 1$) and Surprisal analysis for the populations of NO X $^2\Pi$ ($v = 0, 1$). Relative populations are summed to unity for NO X $^2\Pi$ (v = 0–14). Errors show $\pm 1\sigma$

	NO X $^2\Pi$ (v) vibrational population quenching by N_2O	
v	Direct energy transfer channel	$O(^3P)$ channel
0	0.405 ± 0.111	0.369 ± 0.114
1	0.250 ± 0.069	0.252 ± 0.079
2	0.154 ± 0.060	0.169 ± 0.066
3	0.118 ± 0.020	0.130 ± 0.022
4	0.010 ± 0.011	0.011 ± 0.012
5	0.029 ± 0.008	0.035 ± 0.008
6	0.009 ± 0.004	0.010 ± 0.004
7	0.011 ± 0.002	0.012 ± 0.002
8	0.005 ± 0.001	0.005 ± 0.002
9	0.005 ± 0.001	0.006 ± 0.001
10	0.002 ± 0.001	0.003 ± 0.001
11	0.001 ± 0.001	0.001 ± 0.001
12	0.001 ± 0.001	0.001 ± 0.001
13	<0.001	<0.001
14	<0.001	<0.001

in the others. We also need to consider a highly exothermic reactive channel which does not form NO:

$$\text{NO A } ^2\Sigma^+ (v = 0) + N_2O \rightarrow NO_2 \text{ X } ^2A_1 + N_2 \text{ X } ^1\Sigma_g^+ (v)$$
$$\Delta H^0_{298} = -413.0 \pm 1 \text{ kJ mol}^{-1} \quad (14)$$

In order to find the contribution from unobserved channels, we need to estimate the NO populations in v = 0 and 1 which accompany processes giving the observed higher vibrational levels. This would be straightforward by Surprisal analysis if process (10) dominated, but there are complications because of the potential occurrence of processes (11)–(13) and the fact that for the steps producing three fragments the form of the prior distributions depends upon whether or not the process is concerted or takes place with the nascent N_2O or NO_2 formed above their dissociation limits in processes (9) or (14) then dissociating sequentially to form atomic N or O fragments.[34,35] We first adopt a simple procedure in order to get a qualitative measure of the unobserved channels by treating the vibrational distribution as if it were described by a ''temperature'' and extrapolating the Boltzmann distribution to v = 0 and 1. For the CO_2 data described earlier, such a procedure leads to an estimate of the unobserved channels of 71%, close to the 74% calculated by Surprisal analysis. Using data taken with optical filters we then find that the N_2O unobserved channels (*i.e.* producing no observable NO ($v \geq 2$)) now account for only 2 ± 6% of the total process, *i.e.* zero within the error bars of this analysis, in marked contrast to the 74% estimated for quenching by CO_2.

Process (13) (either direct or sequential) can only produce NO X $^2\Pi$ (v) in $v \leq 2$. We see no marked increase in the population of v = 2 in the overtone spectrum on addition of N_2O, and therefore conclude that (13) is dominantly an unobserved reaction. As in the case of CO_2 we do see nascent emission from vibrationally excited NO_2, implying that process (14) does occur, but again the emission is weak in comparison with that from the NO overtone (considerably weaker than that in the case of CO_2) and we conclude that little partitioning of internal energy into NO_2 occurs in process (14). This argues against the sequential steps (14) followed by dissociation of internally excited NO_2 being the dominant route to formation of the observed vibrationally excited NO. We now carry out Surprisal analyses for processes (10) and (11), with the latter considered as a concerted reaction, and deal with process (12) later. The Prior distribution for the two body dissociation process (10) is given by eqn (6). For the concerted three body dissociation (11) the result is[36]

$$P^0(f_v) = N(1 - f_v)^5 \quad (15)$$

The two Surprisal plots are given in Fig. 9, and the extrapolated populations in v = 0 and 1 listed in Table 2. The Surprisal parameters are 4.7 and 1.0 for processes (10) and (11) respectively, with the percentage of the available energy appearing in vibration in NO being 8.0% for process (10) (statistical would be 11.8%) and 12.9% for process (11) (statistical is 14.3%). From these data we also find that if (10) dominates the observed channels then the unobserved channels are found to account for 7 ± 5% of the total quenching by N_2O: if (11) dominates then this fraction increases to 15 ± 5%.

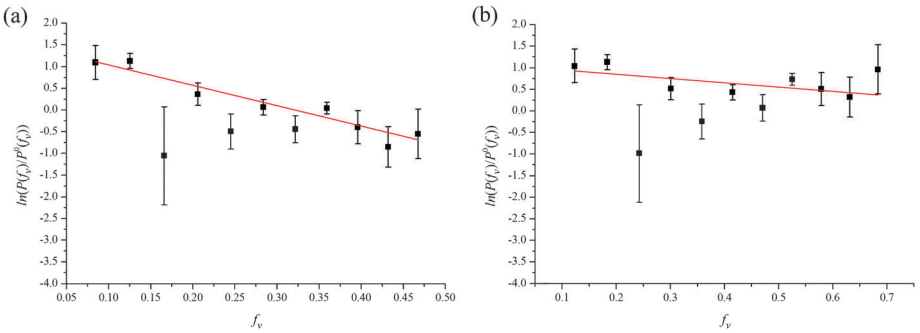

Fig. 9 Surprisal plots of the nascent vibrational distributions of NO X $^2\Pi$ (v = 2–12) following pumping of 50 mTorr NO to the A $^2\Sigma^+$ (v = 0) state in the presence of N_2O. (a) Direct energy transfer from NO A $^2\Sigma^+$ to N_2O, process (10), Surprisal parameter λ_1 = 4.7. (b) Three body concerted dissociation step to form NO X $^2\Pi$ (v), N_2 and $O(^3P)$, as described in process (11), Surprisal parameter λ_1 = 1.0.

We now consider process (12). This can populate up to $v = 8$ in NO, and as populations were observed up to $v = 15$, the process cannot dominate. However it cannot be neglected: the presence of $O(^1D)$ was confirmed by the addition of D_2 resulting in the formation of vibrationally excited OD in reaction (16)

$$O(^1D) + D_2 \rightarrow OD\ X\ ^2\Pi\ (v) + D \qquad (16)$$

and emitting from $v = 1$–4 in the fundamental band near 2600 cm^{-1}, a region not affected by emission from other species. Conditions were chosen such that $O(^1D)$ reacted dominantly with D_2 rather than N_2O (which would produce vibrationally excited NO[37]) yet quenching of NO A $^2\Sigma^+$ by D_2 was negligible. The emission was weak in comparison with that from the NO overtone, and an approximate quantum yield was calculated by comparing intensities of the two emission bands. The calculation requires the vibrational populations of reaction (16)[38] and the Einstein A coefficients for the OD fundamental bands: the latter were obtained by scaling those for the corresponding OH transitions[39] using a $v^3|R|^2$ dependence, where v is the band frequency and $|R|^2$ the square of the transition matrix element (proportional to $\mu^{-1/2}$ where μ is the reduced mass, and thus scaling as v). The quantum yield of $O(^1D)$ was found to be between 2.3 and 2.5% depending upon which set of NO populations in Table 2 was used, a result which clearly indicates that process (12) is a minor one.

The dominant feature of Fig. 7 is the intense emission near 2200 cm^{-1}. This bears a remarkable resemblance both in wavenumber and time dependences to the emission seen following the 193 nm photolysis of N_2O,[37] and which was attributed to the energy transfer process

$$N_2\ X\ ^1\Sigma_g^+\ (v') + N_2O \rightarrow N_2\ X\ ^1\Sigma_g^+\ (v'') + N_2O\ (v_3 = 1) \qquad (17)$$

resulting in emission in the N_2O $\Delta v_3 = -1$ bands. In this case N_2 $X\ ^1\Sigma_g^+\ (v')$ was produced by the 193 nm photolysis of N_2O: here we suggest that process (11) can produce the internally excited N_2. Emission near 2200 cm^{-1} excludes that from N_2O (0,0,1), which would be removed by self absorption, and may be dominantly from N_2O (0,1,1).[37] An alternative route to N_2O excitation, energy exchange with NO (v) is too slow[21] to account for the observed rise time of the signal.

We conclude from this section that our results are consistent with the dominant process for quenching of NO A $^2\Sigma^+$ ($v = 0$) by N_2O being the reactive step (11), which produces ground state NO with a distribution close to statistical. Although we cannot rule out the direct energy exchange process (10) to form vibrationally excited NO, a comparison with the similar processes (1a and 1b) with CO_2 shows that if (10) occurs it takes place with a mechanism that transfers a far lower fraction of the available energy into the internal modes of the triatomic. The dominant long time N_2O emission is from low levels, consistent with formation by vibrational energy exchange with N_2. If process (10) is neglected, then the quantum yield of (11) is *ca.* 85%, with minor processes identified as forming NO_2 and $O(^1D)$.

Discussion

We first compare our results with previous measurements. Settersten *et al.*[16] found a population of NO X $^2\Pi$ ($v = 0$) produced by the quenching of NO A $^2\Sigma^+$ ($v = 0$) by CO_2 of some 60%, considerably higher than the population produced by other quenching partners CO, O_2 and H_2O. Our observations suggest that an upper limit for the quantum yield for NO X $^2\Pi$ ($v = 0$) is the sum of the appropriate fraction of process (1a), 6%, and the sum of the other two major processes, (1b) and (2), 74% giving a total of 80%. A lower value could arise from any NO X $^2\Pi$ ($v = 1$) formed in (1a) and from contributions from (3) and (4). We concur with Settersten *et al.*[16] that the formation of vibrationally unexcited NO X $^2\Pi$ ($v = 0$) is the major process. Cohen and Heicklen[40] employed end product analysis to measure the production of CO following the excitation of NO A $^2\Sigma^+$ ($v = 0, 1$) in the presence of CO_2, and concluded that CO was a major reaction product. More recently Codnia *et al.*[41] have measured end products NO_2 and CO formed in a 1 : 1 ratio following the quenching of NO A $^2\Sigma^+$ ($v = 2$) with CO_2. Under their experimental conditions both processes (2) and (3) would yield these products as recombination of O atoms formed in process (2) with NO would occur. They concluded that 25% of the quenching process takes place by reaction. Although these observations differ markedly, the present data are unable to provide a clear distinction because of the unknown branching ratio of the channels producing unobserved NO X $^2\Pi$ ($v = 0, 1$).

Our conclusions agree with those of Settersten *et al.*[16] that corrections will be required to saturated LIF signals from NO at pressures of CO_2 such that repopulation of the observed ground vibrational state is likely during the excitation pulse. For example, our results indicate that for a mixture of air with 5% CO_2 at atmospheric pressure, some 25% of the excited NO A $^2\Sigma^+$ ($v = 0$) will be returned to the probed NO X $^2\Pi$ ($v = 0$) state by collisions solely with CO_2 in a time of *ca.* 2 ns, shorter than most standard LIF pulses. Although quenching by O_2 returns a smaller fraction of the NO A $^2\Sigma^+$ ($v = 0$) molecules to NO X $^2\Pi$ ($v = 0$) than does CO_2,[16] under the same conditions the process would result in some 20% repopulation of the ground state in this example.

Measurements of the temperature dependence of the quenching rate constants with CO_2[8,11,12] have been used to infer the quenching mechanism. Between 215 K and 520 K the values decrease with increasing temperature, and at higher temperatures achieved in shock tube studies (up to 2400 K), then show a modest increase. The decrease has been explained in terms of formation of a collision complex[8,11,13] and would be in agreement with the statistical distributions observed here in NO, but for both quenching molecules an extra mechanism needs to be invoked to explain the dominance of the reactive channels. The mild increase in quenching rate constant for CO_2 has been explained by a model[42] which allows both collision complex formation and, at higher energies, a charge transfer (harpoon) mechanism leading to the formation of NO^+ and CO_2^-. Both mechanisms are assumed to occur, their fractional importance depending upon the position of the centripetal

barrier to complex formation relative to that of the electron transfer distance R_c (the crossing point of neutral and ionic states).[8] If the harpooning mechanism is ''sudden'', producing NO^+ in $v = 0$, then electron transfer to give NO X $^2\Pi$ would result in vibrational distribution reflecting the NO X $^2\Pi$–NO^+ Franck Condon factors, which peak at low v ($v = 1$ and 2)[16] and thus could contribute to any unobserved NO formed by process (1b), but cannot be dominant in producing $v = 0$ because of the unfavourable Frank–Condon factors. We note however that the applicability of such models to collisional electronic quenching has been called into question.[43] Franck Condon arguments applied to CO_2–CO_2^- would however predict considerable vibrational excitation in all degrees of freedom because of the large geometry change expected between the neutral molecule and the anion.[44] If the ion-pair state crossed immediately to form CO_2 above the barrier to dissociation, process (2) would result. This argument would predict that reaction would dominate at higher temperatures as suggested by Settersten *et al.*[11] A second prediction would be that the distance R_c would be increased by vibrational excitation in NO A $^2\Sigma^+$ and would lead to a higher quantum yield of reaction. Such a process will be investigated in future experiments on the quenching of NO A $^2\Sigma^+$ ($v = 1$) by CO_2.

The occurrence of both reactive and non-reactive quenching processes for another diatomic A $^2\Sigma^+$ state, that of the OH radical, has been extensively studied by Lester and co-workers[45–50] for the colliding partners N_2, CO_2, O_2, H_2 and CO. The quantum yields for non reactive quenching (producing OH in the $v = 0$, 1, and 2 vibrational levels of the ground electronic state, and observed by LIF) depend markedly upon the identity of the colliding molecule, and decrease in the order of the colliders given above from 0.88 for N_2 to zero within experimental error for CO. For the OH + H_2 case the results are able to be compared with classical dynamics calculations on a OH (A, X) + H_2 potential energy surface,[49] with numerous conical intersections identified and being the starting points for the scattering trajectories. Such detailed surfaces however are not available for the NO systems studied here. For the OH A $^2\Sigma^+$ + CO_2 system some 64% of products were found as the non-reactive collisionally quenched OH X $^2\Pi$ ($v = 0,1$) species,[47] but comparison with NO A $^2\Sigma^+$ quenching cannot be made because the dissociative CO_2 channel is not energetically feasible in the OH case.

For quenching by N_2O there are several channels (10)–(13) which could be responsible for the formation of NO X $^2\Pi$ (v), but we consider only processes (10) and (11) to be significant on the grounds that (a) (12) is shown to be minor by O(^{1}D) observation and (b) (13) produces very little vibrationally excited NO_2 and NO ($v = 2$), and cannot have a quantum yield greater than 15% as determined as an upper limit for the unobserved channels. If process (10) dominates it must take place in a fashion very different from that seen for quenching by CO_2 and produce a very low yield of vibrationally excited N_2O. Reaction (11) is favoured both on these grounds and on the indirect observation suggesting the participation of vibrationally excited N_2. The Surprisal parameter resulting from this analysis is 1.0, again suggesting that the NO distribution is close to statistical. As for the CO_2 quenching process, the ground state vibrational distribution suggests complex formation in the quenching mechanism for NO A $^2\Sigma^+$ ($v = 0$).

Conclusions

A comparison between the results found for quenching of NO A $^2\Sigma^+$ ($v = 0$) by CO_2 and N_2O reveals one marked similarity: the observed NO X $^2\Pi$ (v) distributions are all close to statistical, a conclusion also reached for the products of self quenching in a previous study.[17] Although this appears to favour a complex forming mechanism,[8,11,13,44] the results are consistent with the simple energy transfer as given by processes (1a) and (10) being minor channels in both cases. The energy transferred to internal modes of the triatomics is markedly different in the two acceptor molecules, with far more energy appearing in CO_2 than in N_2O. A possible rationalisation is that reaction (11) dominates for collisions with N_2O with (10) being a minor process, but for CO_2, as there is a greater yield of unobserved processes, that either steps (1a) or (1b) could give vibrational excitation in CO_2. If it were process (1a), then the collision complex argument would need modification to account for the greater than statistical fraction of the available energy appearing as triatomic vibration. Although we cannot distinguish between channels (1b) and (2) as being responsible for the high fraction of unobserved NO, it is clear that the processes must compete with energy transfer (1a). For example if a NO–CO_2 complex is formed, as it decomposes, trajectories could favour extension of the C–O bond, with process (2) taking place when little energy is available in NO and when dissociation becomes thermodynamically accessible. This bond extension (or other vibrational excitation in CO_2) appears to persist even when the NO has reached a statistical distribution, and presumably reflects the vibrationally specific exit channels: for example, a T-shaped NO–CO_2 complex could dissociate with NO having a statistical distribution, and the departing O–C–O moiety having an extended O–C bond which cannot transfer vibrational energy to the NO at right angles to it. For N_2O the possibility of bond fission to form O (and to a lesser extent, N) leaves virtually no parent molecule intact. Other reactive channels have been identified for both colliders, but appear to be minor processes. Further experiments are in progress to test some of these conclusions. In particular, quenching of NO A $^2\Sigma^+$ ($v = 1$) by CO_2 is being carried out, with the prediction that channel (2) will become more dominant over the energy transfer step (1), and lead to some direct production of CO ($v = 1$).

Acknowledgements

This work was supported by the EPSRC programme grant EP/G00224X/1: New Horizons in Chemical and Photochemical Dynamics. JF and SG are grateful to the EPSRC for the award of studentships, and MABP thanks the Argentinean Research Council CONICET for funding a one year visiting fellowship to Oxford University.

References

1 N. Georgiev and M. Alden, *Spectrochim. Acta, Part B*, 1997, **52**, 1105–1112.
2 J. B. Nee, C. Y. Juan, J. Y. Hsu, J. C. Yang and W. J. Chen, *Chem. Phys.*, 2004, **300**, 85–92.
3 T. J. McGee, G. E. Miller, J. Burris Jr and T. J. McIlrath, *J. Quant. Spectrosc. Radiat. Transfer.*, 1983, **29**, 333–338.
4 G. D. Greenblatt and A. R. Ravishankara, *Chem. Phys. Lett.*, 1987, **136**, 501–505.
5 J. A. Gray, P. H. Paul and J. L. Durant, *Chem. Phys. Lett.*, 1992, **190**, 266–270.
6 J. W. Thoman Jr, J. A. Gray, J. L. Durant Jr and P. H. Paul, *J. Chem. Phys.*, 1992, **97**, 8156–8163.
7 J. Luque and D. R. Crosley, *J. Chem. Phys.*, 2000, **112**, 9411–9416.
8 R. Zhang and D. R. Crosley, *J. Chem. Phys.*, 1995, **102**, 7418–7424.
9 M. Asscher and Y. Haas, *J. Chem. Phys.*, 1982, **76**, 2115–2126.
10 G. A. Raiche and D. R. Crosley, *J. Chem. Phys.*, 1990, **92**, 5211–5217.
11 T. B. Settersten, B. D. Patterson and J. A. Gray, *J. Chem. Phys.*, 2006, **124**, 234308.
12 T. B. Settersten, B. D. Patterson and C. D. Carter, *J. Chem. Phys.*, 2009, **130**, 204302.
13 P. H. Paul, J. A. Gray, J. L. Durant Jr and J. W. Thoman Jr, *Chem. Phys. Lett.*, 1996, **259**, 508–514.
14 I. S. McDermid and J. B. Laudenslager, *J. Quant. Spectrosc. Radiat. Transfer*, 1982, **27**, 483–492.
15 M. C. Drake and J. W. Ratcliffe, *J. Chem. Phys.*, 1993, **98**, 3850–3865.
16 T. B. Settersten, B. D. Patterson, H. Kronemayer, V. Sick, C. Schulz and J. W. Daily, *Phys. Chem. Chem. Phys.*, 2006, **8**, 5328–5338.
17 G. Hancock and M. Saunders, *Phys. Chem. Chem. Phys.*, 2008, **10**, 2014–2019.
18 S. R. Leone, *Acc. Chem. Res.*, 1989, **22**, 139–144.
19 J. J. Sloan and E. J. Kruus, *''Time Resolved Spectroscopy'' in ''Advances in Spectroscopy''*, Wiley, Chichester, 1989.
20 G. Hancock and D. E. Heard, *Adv. Photochem.*, 1993, **18**, 1–65.
21 G. Hancock, M. Morrison and M. Saunders, *Phys. Chem. Chem. Phys.*, 2009, **11**, 8507–8515.
22 M. Saunders, D. Phil thesis, University of Oxford, 2007.
23 J. Luque and D. R. Crosley, *J. Chem. Phys.*, 1999, **111**, 7405–7415.
24 T. B. Settersten, B. D. Patterson and W. H. Humphries, *J. Chem. Phys.*, 2009, **131**, 104309.
25 R. B. Bernstein, *Chemical Dynamics Via Molecular Beam and Laser Techniques*, Clarendon, Oxford, 1982.
26 J. L. Kinsey, *J. Chem. Phys.*, 1971, **54**, 1206–1217.
27 M. J. Berry, *Chem. Phys. Lett.*, 1974, **29**, 323–328.
28 J. T. Muckerman, *J. Phys. Chem.*, 1989, **93**, 179–184.
29 G. Herzberg, *Molecular Spectra and Molecular Structure, Volume II. Infrared and Raman Spectra of Polyatomic Molecules*, Van Nostrand Reinhold, New York, 1945.
30 D. Bailly, R. Rarrenq, G. Guelachvili and C. Rossetti, *J. Mol. Spectrosc.*, 1981, **90**, 74–105.
31 R. A. Brownsword and G. Hancock, *J. Chem. Soc., Faraday Trans.*, 1997, **93**, 1279–1286.
32 B. Bohn, A. Doughty, G. Hancock, E. L. Moore and C. Morrell, *Phys. Chem. Chem. Phys.*, 1999, **1**, 1833–1842.
33 L. A. Pugh and K. N. Rao, *Intensities from infrared spectra, Molecular spectroscopy: Modern research*, Academic Press, New York, 1976, Vol. II.
34 C. E. M. Strauss and P. L. Houston, *J. Phys. Chem.*, 1990, **94**, 8751–8762.
35 C. Maul and K.-H. Gericke, *Int. Rev. Phys. Chem.*, 1997, **16**, 1–79.
36 H. Sekiya, N. Nishiyama, M. Tsuji and Y. Nishimura, *J. Chem. Phys.*, 1987, **86**, 163–169.
37 G. Hancock and V. Haverd, *Phys. Chem. Chem. Phys.*, 2003, **5**, 2369–2375.
38 Y. Liu, Y. Gao, D. Shi and J. Sun, *Chem. Phys.*, 2009, **364**, 46–50.
39 D. N. Turnbull and R. P. Lowe, *Planet. Space Sci.* 1989, **37**, 723–738.
40 N. Cohen and J. Heicklen, *J. Phys. Chem.*, 1967, **71**, 558–563.
41 J. Codnia, F. A. Manzano and M. L. Azcárate, *J. Photochem. Photobiol., A*, 2011, **223**, 65–69.
42 P. H. Paul, J. A. Gray, J. L. Durant Jr and J. W. Thoman Jr, *Appl. Phys. B: Photophys. Laser Chem.*, 1993, **57**, 249–259.
43 M. H. Alexander and G. C. Corey, *J. Chem. Phys.*, 1986, **84**, 100–113.
44 K. O. Hartman and I. C. Hisatsune, *J. Chem. Phys.*, 1966, **44**, 1913–1918.
45 P. A. Cleary, L. P. Dempsey, C. Murray, M. I. Lester, J. Kłos and M. H. Alexander, *J. Chem. Phys.*, 2007, **126**, 204316.
46 L. P. Dempsey, C. Murray, P. A. Cleary and M. I. Lester, *Phys. Chem. Chem. Phys.*, 2008, **10**, 1424–1432.
47 L. P. Dempsey, T. D. Sechler, C. Murray and M. I. Lester, *J. Phys. Chem. A*, 2009, **113**, 6851–6858.
48 L. P. Dempsey, T. D. Sechler, C. Murray, M. I. Lester and S. Matsika, *J. Chem. Phys.*, 2009, **130**, 104307.
49 J. H. Lehman, L. P. Dempsey, M. I. Lester, B. Fu, E. Kamarchik and J. M. Bowman, *J. Chem. Phys.*, 2010, **133**, 164307.
50 J. H. Lehman, M. I. Lester and D. R. Yarkony, *J. Chem. Phys.*, 2012, **137**, 094312.